scientific reports



OPEN

The E193K LRRK2 mutation interferes with the autophagosome processing through the impairment of the LRRK2-Dynein-1 complex

Stefan Redl¹, Felix Von Zweydorf², Christian J. Gloeckner², Inmaculada Posadas^{3,4}, Valentín Ceña^{3,4}, Michael W. Hess⁵, Giovanni Piccoli⁶ & María Dolores Pérez-Carrión^{3,4⊠}

Parkinson's disease (PD) is a neurodegenerative pathology characterized by movement-associated symptoms due to the selective loss of dopaminergic neurons in the substantia nigra pars compacta. Autophagy is an essential mechanism that restores homeostasis and promotes cell survival. Mutations in the Leucine-Rich Repeat Kinase 2 (LRRK2) gene are among the most common in the familial cases. The LRRK2 E193K mutation falls in the Armadillo (ARM) domain and modifies LRRK2 interactome. The role of LRRK2 in autophagy has been widely explored, but the impact of E193K mutation on autophagy remains unknown. We found that the E193K variant increases autophagy in primary fibroblasts obtained from an E193K carrier. By cryo-based electron microscopy we observed that E193K fibroblasts present a higher amount of phagophores/autophagosomes. We showed that LRRK2 binds to the Dynein-1 complex, an essential regulator of retrograde transport of autophagosomes. Noteworthy, the E193K mutation jeopardizes this interaction and increases the cellular sensitivity to 1-methyl-4-phenylpyridinium (MPP+) toxin in fibroblasts as well as in a heterologous cell model. Our study reveals that the LRRK2 E193K variant influences the autophagic regulation and suggests that the dysregulation of the LRRK2-Dynein-1 complex causes autophagic defects and, eventually, cell death.

Keywords Parkinson's disease, LRRK2 protein, Dynein-1 complex, Autophagy, Ultrastructure, Organelle morphometry

Parkinson's disease (PD) is a chronic, progressive and disabling neurodegenerative pathology with a variable onset, between 45 and 70 years¹. The number of patients affected by PD has doubled in the last 20 years and it will reach 12 million worldwide by 2040, becoming the second most common aged-related neurodegenerative disorder². Clearly, there is an urgent need for effective therapeutic options to modify both the onset and the evolution of the disease³. The clinical PD diagnosis depends on the characterization of several movement-associated symptoms, such as tremor, slowed movements and postural instability. These symptoms worsen with longevity and the progression of the disease. Patients are frequently affected by non-motor manifestations, including cognitive impairment, depression, sleep disorders, and gastrointestinal or olfactory alterations⁴. The physiopathology of PD is mainly related to the dopamine deficiency in the striatum due to the selective loss of dopaminergic neurons in the substantia nigra pars compacta (SNpc).

The etiology of PD is complex and reflects the interaction among ageing, genetic, and environmental factors⁵. Indeed, neuronal death is precipitated by the exposure to toxic substances such as pesticides (rotenone or paraquat), dithiocarbamates or organochlorines. Accordingly, the administration of MPP⁺ toxin, an active metabolite of 1-methyl-4-phenyl-1,2,3,6-tetrahydropyridine (MPTP), recapitulates PD in both in vitro and in vivo models⁶. Although most PD cases are considered sporadic forms (~ 84% of the cases), the identification of more than 90 genes and loci associated with PD susceptibility and familial cases linked to specific mutations confirmed the relevance of genetics in the disease onset^{7,8}. Among PD-genetic causes, mutations in the gene encoding Leucine-Rich Repeat Kinase 2 (LRRK2) protein are the most frequent⁹. LRRK2 is a multi-domain protein with two scaffolding terminal domains that orchestrate LRRK2-protein interactions^{10,11}. LRRK2

¹Institute of Neuroanatomy, Innsbruck Medical University, Innsbruck, Austria. ²German Centerfor Neurodegenerative Diseases (DZNE), Tübingen, Germany. ³CIBER, Instituto de Salud Carlos III, Madrid, Spain. ⁴Unidad Asociada Neurodeath, INAMOL, Universidad de Castilla-La Mancha, Albacete, Spain. ⁵Institute of Histology and Embryology, Innsbruck Medical University, Innsbruck, Austria. ⁶CIBIO, Università degli Studi di Trento, Trento, Italy. [™]email: mariad.perez@uclm.es

organizes a complex signaling network lying at the core of different pathways and cellular structures including synaptic vesicles, endo-lysosomal and autophagic compartments, mitochondria and the cytoskeleton¹². The biological function of LRRK2 is hampered by different missense mutations in the LRRK2 gene. LRRK2 single nucleotide polymorphisms (SNPs) are responsible for 2–5% of familial PD cases with autosomal dominant inheritance, and they are recognized as a common risk factor even in sporadic forms, accounting for 1% up to 2% of cases^{13,14}. Among the different mutations, the G2019S substitution is the best characterized and the most frequent in both sporadic and familial PD cases¹⁵. Genetic studies have identified less explored pathological variants falling outside the enzymatic domains of LRRK2. That applies to the E193K substitution we identified in 3 siblings of a non-consanguineous Italian family¹⁶- to our knowledge the only cases reported so far. The E193K variant is an extremely rare mutation responsible for PD onset around 45 years old. Although the substitution of glutamic acid for lysin in LRRK2 sequence does not affect kinase activity, this mutation modifies LRRK2 protein folding and interactome, thus affecting both mitochondrial dynamics and synaptic vesicle trafficking^{16,17}.

Macroautophagy (autophagy, hereinafter) is a fundamental mechanism to eliminate aberrant cellular compounds and restore homeostasis in both healthy and pathological situations^{18,19}. This dynamic multi-step pathway involves the engulfment of damaged organelles or aggregated proteins in unique, double-membrane vesicles called autophagosomes and eventually, their degradation via fusion with endosomes²⁰ and/or the lysosomes^{19,21}. Cumulating evidence demonstrates the role of LRRK2 in autophagy^{22–25}. Although the effects of several LRRK2 mutations in autophagy have been described^{23,24}, the impact of the E193K mutation on autophagic processes is still unknown.

Nascent autophagosomes generally move centripetally along the microtubule cytoskeleton for subsequent fusion with endosomes and/or lysosomes, though the specific molecules and mechanisms involved do vary in detail depending on cell type^{21,26–28}. Coordinated vectorial movements of all those organelles are essential for efficient organelle encounters leading finally to autolytic clearance; this is particularly challenging in the uniquely shaped, polarized neurons because of the highly differential distributions of autophagosomes, forming in the distal axon and perinuclear endo/lysosomes in the soma²⁹. The retrograde movement of autophagosomes is sustained by molecular motors as the Dynein 1 (Dyn-1) complex^{27,30}. Dyn-1 is a homodimer composed by a motor domain, the Dynein-1 heavy chains (Dyn-1 HC), and a tail domain formed by multiple accessory chains as Dynein-1 intermediate chains (Dyn-1 IC), Dynein light-intermediate chains (Dyn-1 LIC) and Dynein light chains (dyn-1 LC)³¹. It is known that isolated LRRK2 catalytic domains interact with microtubules and block Dyn-1 transport³², but it is not clear whether PD mutations interfere with LRRK2-Dyn-1 complex and autophagosome mobility.

In the present study we focused on the impact of the E193K LRRK2 variant on autophagy and on the response to MPP $^+$ neurotoxin. Moreover, we investigated the effect of the E193K mutant on the LRRK2 Dyn-1 complex. As a cell model, we used primary skin fibroblasts derived from one patient carrying this E193K mutation 16 , the only patient samples available so far with this variant.

Materials and methods Cell cultures and treatments

Human control and E193K PD primary fibroblasts were provided by the Telethon Cell Line and DNA Biobank from patients affected by Genetic Diseases (protocol #1339) at passages 1–2. Cells had been prepared by skin biopsy gathered from one PD patient carrying the E193K LRRK2 mutation and one age and sex-matched healthy control patient, as previously described 16 . Cells were grown in culture medium composed by Dulbecco's Modified Eagle Medium (DMEM) (DMEM-HPXA, Capricorn Scientific) supplemented with 20% Fetal Bovine Serum (FBS) (FBS-11 A, Capricorn Scientific), 1% L-glutamine (SH30852.0, Cytiva) and 1% Penicillin/Streptomycin (PS-B, Capricorn Scientific). Cells were used for all experiments until 15 passages in vitro. HEK293 cells (ATCC CRL-1573) were grown in culture medium prepared with DMEM medium supplemented with 10% FBS, 1% L-glutamine and 1% Penicillin/Streptomycin. Both human fibroblasts and HEK293 cell line were maintained at a density of 2 \times 10 6 cells in a 100 mm cell culture dish (Sarstedt) and incubated at 37 °C in a saturated humidity atmosphere containing 5% CO $_2$ and passaged once or twice in a week using Trypsin-EDTA 0,05% (TRY-4B, Capricorn Scientific).

Cellular treatments were performed, when indicated, by adding MPP⁺ iodide (1mM), NH₄Cl (5mM) or fresh cell culture medium for 24 h or the specific indicated time period. NH₄Cl (A9434) and MPP⁺ iodide (D048) were purchased from Sigma-Aldrich-Merck.

Plasmids and transfection

Full-length wild-type Strep-FLAG-hLRRK2 construct was previously described 33,34 , while E193K variant was generated by site-directed mutagenesis using the Quick-change Mutagenesis kit (Stratagene, Sigma-Aldrich). Strep-FLAG LRRK2 construct lacking 1–912 aa at the N-terminal part (named as Δ -Nter) was produced by PCR from the LRRK2 cDNA and cloned into pDEST Strep-FLAG (N-SF-TAP) plasmid as already described 16. Strep-FLAG LRRK2 vector composed by aa 1–2141 and lacking the WD40 domain (named as Δ -WD40) was previously generated 35. GFP-mCherry-LC3B vector was purchased from Addgene (#123230). HEK293 cells were transfected by using polyethylenimine (PEI) reagent (43896, Alfa Aesar) and specific vectors and processed after 48 h. Human fibroblasts transfection was performed with Amaxa Basic Nucleofector System (Lonza) as previously mentioned 16. Briefly, each transfection was performed by resuspending 1 × 106 fibroblasts in 100 μ L of Nucleofector Solution for mammalian cells (Lonza) and mixed with 3 μ g of GFP-mCherry-LC3 plasmid. Nucleofection was performed using the A33 program on the Amaxa apparatus. Then, 500 μ L of fibroblasts culture medium were added to the cuvette and 1 × 106 fibroblasts were plated on 12-mm coverslips for 24 h before NH₄Cl treatment.

Pull-down assay, co-immunoprecipitation and western-blotting

For the pull-down experiments, 48 h after transfection HEK293 cells were solubilized in lysis buffer (150mM NaCl, 50mM Tris-HCl, 2mM EDTA, 1% NP-40 and 0.25% sodium deoxycholate, pH 7.4) containing protease inhibitors (539131, Calbiochem) for 1 h at 4 °C. LRRK2 was immobilised using Strep-Tactin Superflow Resin (2–1208-010, Iba) for 2 h at 4 °C. Then, resin was washed three times with a high salt buffer (300mM NaCl, 50mM Tris-HCl pH 7.4) and interacting proteins were eluted in Laemmli buffer 2X at 55 °C for 10 min and evaluated by Western-blot assay.

For the immunoprecipitation assays, $4\,\mu g$ of rat anti-LRRK2 (LANK/24D8 clone, provided by Dr. Gloeckner) antibody or rat anti-IgG (sc-2026, Santa Cruz Biotechnology) were incubated with 1 mg of mouse adult brain lysate and loaded onto protein G-Agarose resin (193258, Abcam). Then, resin was washed three times with high salt buffer (300mM NaCl, 50 mM Tris-HCl pH 7.4) and samples were eluted with Laemmli buffer 2X for 10 min at 55 °C. Co-immunoprecipitated proteins were evaluated by Western-blot assay.

For the Western blotting analysis of protein content, human fibroblasts and HEK293 cells were lysed with lysis buffer (150mM NaCl, 2mM EDTA, 50 mM Tris-HCl, 1% NP-40 and 0.25% sodium deoxycholate, pH 7.4) completed with protease inhibitors (539131, Calbiochem), for 1 h at 4 °C. Protein concentration was measured using BCA-Pierce method (Thermo Scientific), following the manufacturers' instructions. For protein analysis by Western blotting, 10-30 µg of total proteins were loaded onto 8-15% Tris-SDS-PAGE gels. After electrophoresis proteins were transferred onto PVDF membrane (162 - 0115, Bio Rad) in semi-dry conditions at 250 mÅ for 90 min. In all experiments, the primary antibodies were applied overnight in blocking buffer (20mM Tris, pH 7.4, 150mM NaCl, 0.1% Tween 20, and 5% non-fat dry milk). Primary antibodies included: rabbit anti-LRRK2 1:500 (133474 Abcam), rabbit anti-p62 1:1000 (5114, Cell Signalling), rabbit anti-LC3 1:500 (NB100-2220, Novus), mouse anti-Dynein IC 1:1000 (s-13524, Santa Cruz), mouse anti-LAMP2 (sc-18822, Santa Cruz), mouse anti-Rab7 (sc-376362, Santa Cruz), mouse anti-Tubulin 1:5000 (CP06, Calbiochem) and rabbit anti-GAPDH 1:3000 (0411, Cell Signalling). Membranes were washed three times for 10 min with TBS-Tween buffer. The secondary antibodies HRP-conjugated anti-rabbit (P0448, Dako) or anti-mouse (P0447, Dako) were used at 1:5000 dilution in blocking buffer. Proteins were detected using the chemiluminescent reagent (42582, Serva). Images were acquired with a manual acquisition system (Fujifilm) and protein quantification was performed by densitometric analysis of the specific bands using the ImageJ software (V1.53a) (NIH Image, https://imagej.net).

Cell viability assay

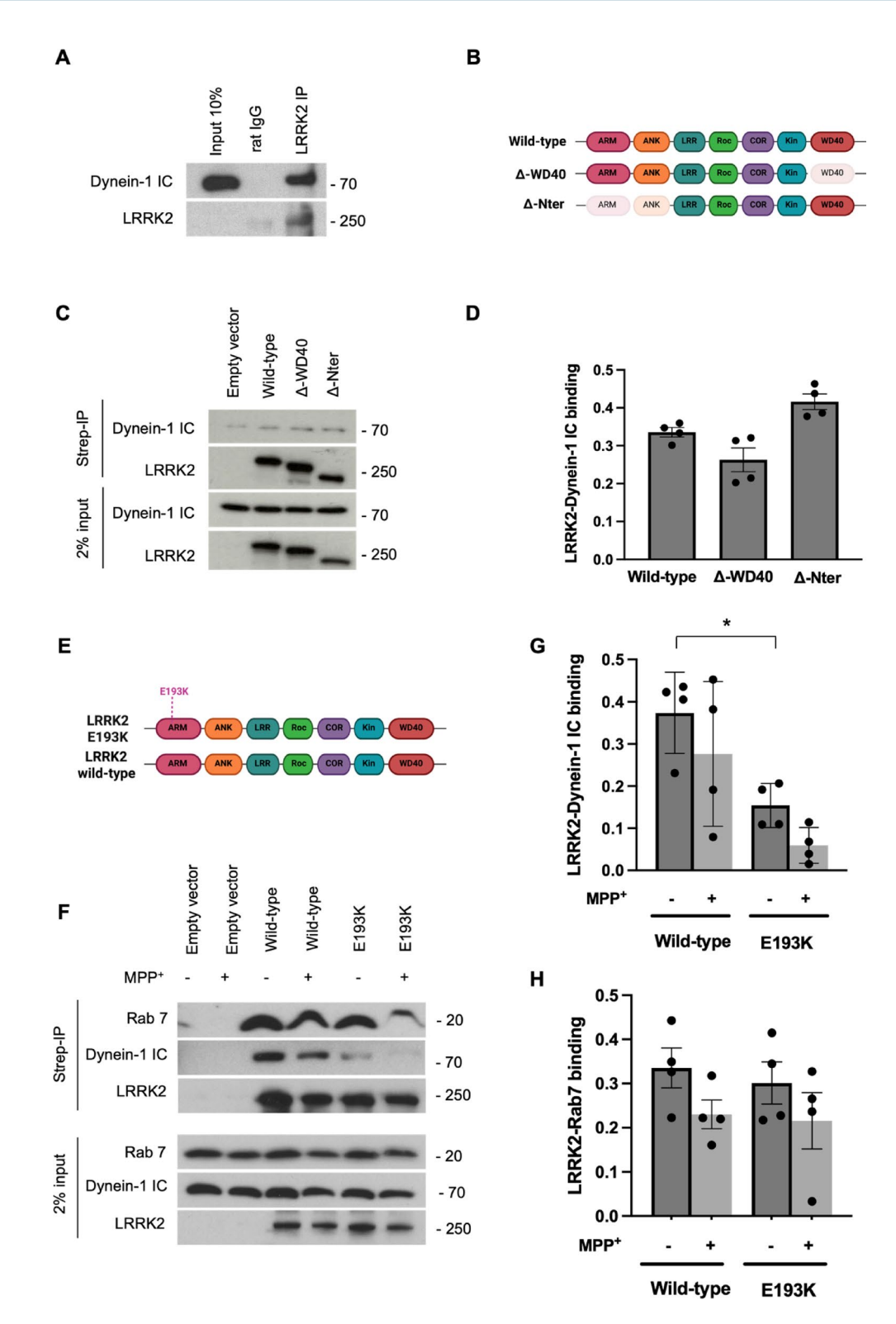
Cell viability was evaluated by measuring Lactate Dehydrogenase (LDH) release into the cellular culture medium as previously described³⁶. Human fibroblasts were seeded in 24 well plates (Sarstedt) at a cellular density of 100,000 cells/mL and incubated for 24 h. After treatment with MPP+ (1mM), cell culture media were collected, and cells were washed with phosphate buffered saline (PBS) and lysed using Triton X-100 (T-9284, Sigma) (0.9% v/v) in PBS. LDH activity, both in culture medium and cellular lysates, was measured using the kit CytoTox 96 Non-radiactive Cytotoxicity Assay (G-1782, Promega) at 490 nm, using a microplate reader (BioRad). Cellular viability was expressed as the percentage of LDH released to the culture medium compared to total LDH amount (expressed as LDH amount in cell lysates plus LDH released to the culture medium).

Fluorescence microscopy

Human primary fibroblasts were transfected by electroporation with the GFP-mCherry-LC3B construct and seeded on 12-mm coverslips for 24 h. Then, cells were treated with NH $_4$ Cl (5mM) for 24 h and fixed with 4% paraformaldehyde for 10 min at room temperature. Coverslips were mounted with FluorSave^{∞} Reagent (Millipore) and analyzed with the epifluorescence microscope ZEISS AXIO IMAGER M2 using a 40x objective, camera settings of 0.102 μ m x 0.102 μ m pixel size. The number of mCherry- and/or GFP-positive puncta per cell profile as seen in single focal planes were counted using ImageJ software (V1.53a) (NIH Image, https://imagej.net).

Electron microscopy

For sample preparation we employed rapid cryofixation through means of high-pressure freezing, freeze substitution and epoxy resin embedding as previously described 16,37, instead of conventional chemical fixation (Supplementary Figure S1A and S1B). The obtained superior ultrastructure preservation allowed a more precise delineation of the individual organelle contours and better distinction of the organelles' internal morphology. This facilitated organelle classification —an essential advantage for quantitation. Cells were cultured for 3 days on sapphire discs, optionally treated with NH₄Cl and processed as described¹⁶. Ultrathin epoxy resin sections (approx. 100nm thick) were analyzed with a CM120 transmission electron microscope (Philips, Eindhoven, The Netherlands) equipped with a MORADA G1 digital camera (EMSIS, Münster, Germany). Processing of digital electron micrographs was optionally carried out with Adobe Photoshop V.9, including adjustment of contrast and brightness, gray-scale modification, sharpening, median and high-pass filtering. For a provisional classification of autophagic organelles we distinguished between phagophores plus autophagosomes (pooled), autolysosomes (including amphisomes), multivesicular late endosomes³⁸ and lysosomes, referring largely to the terminology presented by Holzbaur and colleagues³⁹. To refine quantification we tentatively distinguished bona fide immature from mature, degradative autolysosomes³⁹ based mainly on morphology, including serial section analysis. Autolysosomes were considered (i) as immature, when housing at least one structurally clearly intact, undigested, membrane-bound subcompartment/area inside; (ii) as mature/degradative, when all their (membranous) contents appeared partly or largely digested; (iii) as lysosomes, when highly disintegrated, compacted membrane remnants, opaque inclusions and/or virtually amorphous organelle matrix predominated (Supplementary Figure S2). For thorough morphometry of autophagic and endo-lysosomal organelles we analyzed ≥ 18 cell profiles cut parallel to the substrate and running roughly through the cell center (n = 3



independent cell culture experiments for each genotype/condition, with ≥ 3 technical replicates each). This corresponded to at least 170 digital micrographs (taken at a primary microscope magnification of x11.500) per genotype/condition. Measurement tools of the iTEM software (iTEM V.5.0.0., analySIS Image Processing, from EMSIS, Münster, Germany) were used for point counting, length and area measurements.

Statistical analysis

Data are expressed as the mean value ± standard error of the mean (SEM). All data were analyzed using the Prism GraphPad software (V10, GraphPad, USA). We applied an unpaired Student's t-test (two classes), one-way ANOVA followed by Tukey's post hoc test or two-way ANOVA followed by Sidak's comparisons test (more than two classes). The statistical analysis, the number of experiments (n) and the level of significance (p) values are reported in the figure legends. P values smaller than 0.05 were considered significant.

▼Fig. 1. LRRK2 interacts with Dynein-1 complex and E193K variant impairs LRRK2-Dynein-1 IC interaction. (A) Immunoprecipitation of LRRK2 protein from adult mouse forebrain. Brain extracts were incubated with rat IgG or anti-LRRK2 antibody and immunocomplexes were precipitated with protein G-Agarose beads. LRRK2-Dyn-1 IC interaction was analyzed by Western-Blot. (B) Representation of Strep-FLAG-LRRK2 constructs. (C) HEK293 cells where transfected with strep-FLAG-empty vector, strep-FLAG-LRRK2 wild-type, strep-FLAG-LRRK2 Δ-WD40 (Δ-WD40) and strep-FLAG-LRRK2 Δ-Nterminal (Δ-Nter) for 48 h. Strep-FLAG-LRRK2 variants were isolated on streptavidin resin and interacting proteins were resolved by Western-Blot using anti-LRRK2 and anti-Dyn-1 IC antibodies. (D) The graph represents the extent of Dyn-1 IC binding to LRRK2 by quantification of the amount of Dyn-1 IC protein co-precipitating with LRRK2 wild-type, LRRK2 Δ-WD40 and LRRK2 Δ-Nter. Data are expressed as mean ± SEM; n=4 (E) Representation of Strep-FLAG LRRK2 wild-type and Strep-FLAG LRRK2 E193K variant. (F) HEK293 cells overexpressing strep-FLAG-empty vector, strep-FLAG-LRRK2 wild-type or strep-FLAG-LRRK2 E193K variant were treated with MPP+ (1mM, 24 h), when indicated. Cellular lysates were processed for streptavidin isolation of immunocomplexes, which were evaluated by Western-Blot using anti-LRRK2 and anti-Dyn-1 IC antibodies. (G) The graph reports the extent of Dyn-1 IC binding to LRRK2 by quantification of the amount of Dyn-1 IC protein co-precipitating with strep-FLAG LRRK2 variants. Data are expressed as mean \pm SEM; n = 4. *p < 0.05 Two-way ANOVA. ($\dot{\mathbf{H}}$) The graph reports the extent of Rab 7 interaction to LRRK2 by measuring the amount of Rab7 protein coprecipitating with strep-FLAG LRRK2 variants. Data are expressed as mean \pm SEM; n = 4.

Results

E193K variant disrupts LRRK2-Dynein-1 IC interaction

LRRK2 is a hub for protein interactions ^{10,40}. LRRK2 interacts with microtubules ⁴¹ and the isolated LRRK2 catalytic region interferes with motor proteins as kinesin and dynein ³². In order to expand the LRRK2 interactome, we explored the LRRK2 association to the Dyn-1 complex. We validate the LRRK2-Dyn-1 IC interaction by an immunoprecipitation assay of endogenous LRRK2 protein from adult mouse brain lysate (Fig. 1A). LRRK2 structure includes two platforms typically involved in protein-protein interactions, the N-terminal armadillo (ARM), ankyrin and Leucin Rich Repeat (LRR) domains and the WD40 domain at the C-terminus ⁴². To map the regions of LRRK2 responsible for the interaction with Dyn-1 IC, we overexpressed Strep-FLAG LRRK2 full-length wild-type (wild-type), Strep-FLAG LRRK2 missing the C-terminal WD40 domain (Δ-WD40) and Strep-FLAG LRRK2 construct lacking the N-terminal fragment (Δ-Nter) (Fig. 1B) in HEK293 cells. After streptavidin pull-down, we studied LRRK2-Dyn-1 IC interaction by Western-Blot. We found that both WD40 and N-terminal domains interact with Dyn-1 IC protein (Fig. 1C and D).

Previously, we demonstrated that the E193K variant alters LRRK2 binding properties ^{16,17}. Thus, we investigated whether E193K LRRK2 mutation modified LRRK2-Dyn-1 complex formation. To this aim, we isolated Strep-FLAG-LRRK2 wild-type and Strep-FLAG-LRRK2 E193K mutant (Fig. 1E) upon overexpression in HEK293 cells. Although Dyn-1 IC protein expression was similar in wild-type and E193K samples, we noticed that the wild-type form associates specifically to Dyn-1 IC, while E193K mutation hampered the interaction between LRRK2 and Dyn-1 IC (Fig. 1F and G). PD has a multifactorial origin resulting from the combination of genetic susceptibility and exposure to environmental toxins, such as MPP⁺⁴³. On this matter, the latest hypothesis regarding the development of PD suggests the involvement of several contributing elements such as facilitators, including genetic predisposition and triggers like toxic agents⁴⁴. Therefore, we assessed whether the neurotoxin MPP⁺ could influence LRRK2-Dyn-1 IC interaction and we observed that MPP⁺ exposure did not alter the affinity of either LRRK2 wild-type or E193K for Dyn-IC or Rab7, a key regulator of autophagy⁴⁵ (Fig. 1F, G and H). This finding suggests that the E193K mutation influences the stability of the Dyn-1 IC-LRRK2 complex.

E193K LRRK2 mutation affects autophagy

Both LRRK2 and dynein complex play a critical role in the autophagic-lysosomal pathway⁴⁶. In particular, the dynein complex allows the retrograde transport of autophagosomes⁴⁷ and PD-LRRK2 mutations modify basal autophagy²⁵. To monitor autophagy, several complementary methods have been established⁴⁸. We applied microscopy techniques to study autophagy in our human fibroblast model. Qualitative and quantitative electron microscopy (Fig. 2A, B and C) was performed on rapidly cryofixed samples. The operational organelle classification is described in the Material and Methods section and Supplementary Figure S2. Subcellular characteristics of wild-type and E193K primary fibroblasts, as well as morphometry of autophagic and endolysosomal organelles are illustrated and summarized in Fig. 2A, B and C (see also Supplementary Figure S1B and S2). In baseline conditions frequencies of autophagosomes/phagophores, immature and mature autolysosomes as well lysosomes were quite similar in both genotypes (Fig. 2A, B and C). However, only E193K fibroblasts showed a significantly increased number of autophagosomes/phagophores and immature autolysosomes upon treatment with the lysosomal inhibitor NH₄Cl⁴⁹. Mature autolysosomes accumulated to a similar extent in both genotypes after lysosomal blocking, frequencies of lysosomes remained almost stable. The amount of multivesicular late endosomes remained almost stable upon NH₄Cl exposure in wild-type controls, but doubled in E193K cells (Fig. 2A and C), indicating alterations of the endolysosomal pathway as well.

Thus, electron microscopic observations on the entire autophagic and lysosomal population of untransfected fibroblasts clearly showed enhanced autophagy in E193K fibroblasts. In addition, they strongly suggested, in both genotypes, functional organelle maturation at least up to the stage of mature, degradative autolysosomes, presumably corresponding to functional autophagic flux/turnover. Yet, conclusions on subsequent steps of autophagy, thus, efficiency and progression of (auto)lysosomal degradation were not possible from those experiments.

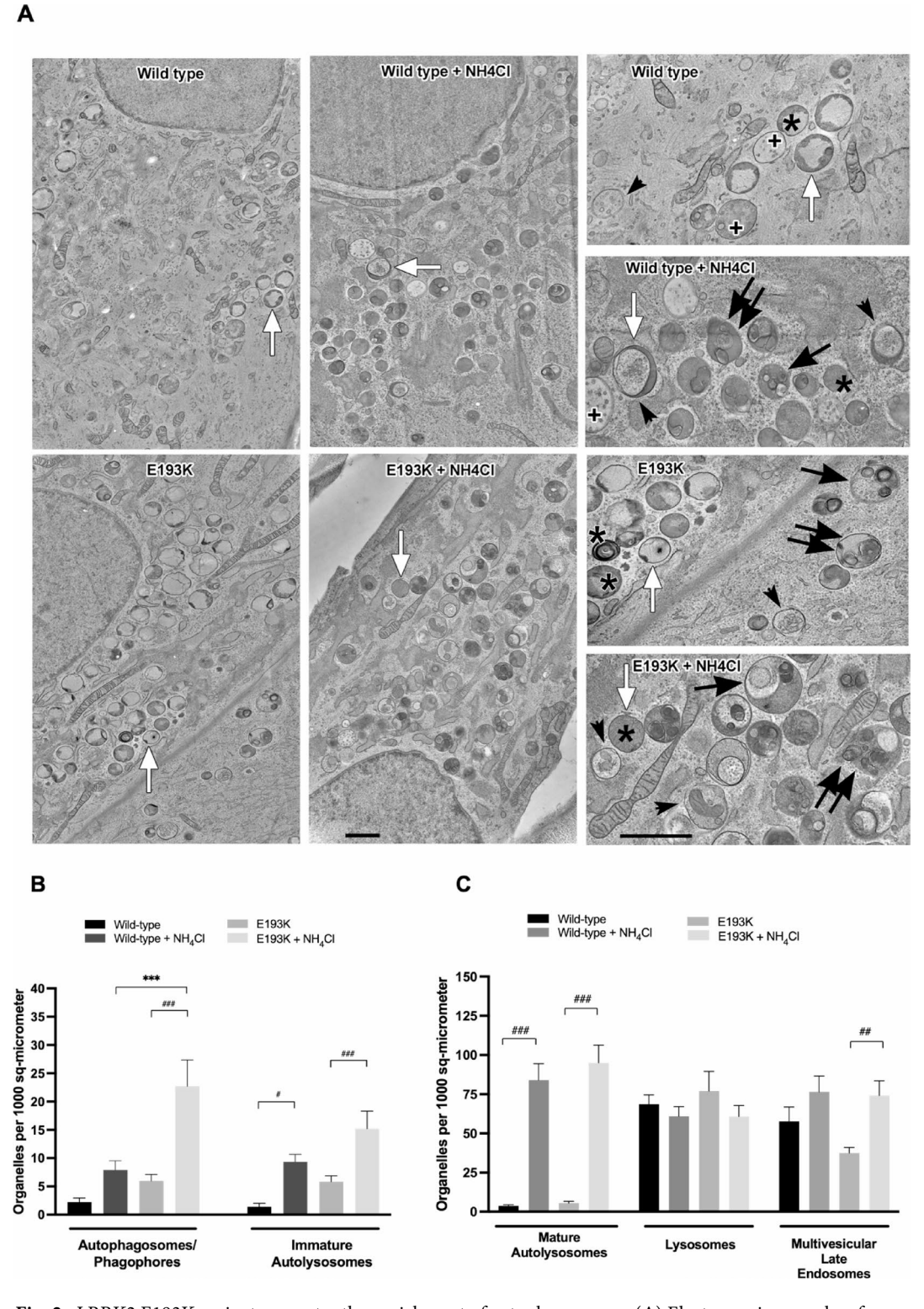


Fig. 2. LRRK2 E193K variant promotes the enrichment of autophagosomes. (**A**) Electron micrographs of autophagic organelles from cryo-fixed human fibroblasts from wild-type and E193K carriers at steady state or upon exposure to NH₄Cl (5mM, 24 h). For explanations of organelle lettering, see Supplementary Figure S2; autophagosome = arrow-heads, multivesicular late endosome = cross, lysosome = asterisk, immature autolysosome = arrow, degradative autolysosome = double arrows; white arrows mark corresponding organelles in the overviews (left and middle rows) and the respective enlarged frames (right row). Scale bars = 1 μ m. (**B**) Ultrastructural morphometry of relative frequencies (per 1000 square micrometer) of early maturation stages of autophagic organelles: autophagosomes/phagophores pooled and immature autolysosomes and (**C**) Ultrastructural morphometry of relative frequencies (per 1000 square micrometer) of mature, degradative autolysosomes, lysosomes and multivesicular late endosomes. Data are expressed as mean ± SEM, n = 3 (6–8 cells for each experiment). ***p < 0.001, **p < 0.05, **p < 0.01, **p < 0.001. Two-way ANOVA.

To complement these observations, we studied autophagy by exploiting the fluorescent reporter GFP-mCherry-LC3B. This reporter emits simultaneously GFP and mCherry fluorescence when the protein localizes in non-acidic structures as the autophagosomes. By contrast, the emission of only the red fluorescence indicates that LC3B is located in acidic, degradative autolysosomes, where the GFP signal is quenched⁵⁰. Accordingly, we transiently expressed the GFP-mCherry-LC3B reporter in wild-type and E193K primary fibroblasts for 48 h and treated the cells with NH₄Cl (5mM) for the last 24 h. Treating cells with NH₄Cl (5mM) caused a significant enrichment of those early maturation stages of autophagic organelles in both wild-type and E193K LRRK2 cells. However, compared to wild-type cells, E193K LRRK2 fibroblasts showed a significantly higher number of yellow puncta, thus, mostly autophagosomes (Supplementary Figure S3). The number of red puncta, i.e., degradative autolysosomes newly formed upon transfection, clearly increased in wild-type fibroblasts as a result of NH₄Cl administration, but slightly decreased in E193K cells (Supplementary Figure S3).

Taken together, our complementary light and electron microscopic data indicate enhanced autophagy in E193K variant expressing cells.

MPP* treatment induces cell death in human fibroblasts

We have previously reported that LRRK2 E193K influences mitochondrial dynamics and response to mitochondrial toxins¹⁶. Thus, we assessed the impact of a prolonged MPP⁺ toxin exposure on cellular viability. To this aim, we treated wild-type and E193K fibroblasts with MPP⁺ toxin (1mM) up to 120 h. We evaluated cell viability by measuring lactate dehydrogenase (LDH) release to the culture medium (Fig. 3). MPP⁺ treatment triggered cell death in both wild-type and LRRK2 E193K cells after 96 h and 120 h of exposure. Noteworthy, we observed that cell death was significantly higher in E193K LRRK2 cells than in controls upon long time incubation (> 96 h). These findings confirmed that the E193K variant increases the sensitive toward MPP⁺ toxin.

MPP* exposure activates autophagy only in wild-type fibroblasts

MPP+ insult can trigger a compensatory autophagic response⁵¹. First, we assessed autophagy in control conditions based on the peculiar migratory features upon Sodium Dodecyl Sulfate-Polyacrylamide Gel Electrophoresis (SDS-PAGE) of the microtubule-associated protein 1 Light Chain 3B I (LC3BI, cytosolic) and II (LC3BII, bound to autophagic membranes) isoforms^{48,52}. We monitored LRRK2 expression, LCBII levels, LC3BII/LC3BI ratio, and LC3BII degradation, assessed according to⁵³, in baseline conditions and in the presence of the lysosomal inhibitor NH₄Cl⁴⁹, (Supplementary Figure S4). Notably, we noticed that LC3BII degradation decreased in E193K LRRK2 cells (Supplementary Figure S4D). The levels of P62, as an autophagic adaptor, can be evaluated to assess autophagic activity⁵⁴. We noticed that P62 protein expression was higher in E193K fibroblasts compared to wild-type fibroblasts in basal conditions (Supplementary Figure S4). To investigate the effect of MPP+ on autophagy in our experimental model, we exposed wild-type and E193K human fibroblasts to 1mM MPP+ for 24 h, i.e. a treatment that did not induce overt toxicity. As expected, MPP+ treatment enhanced LC3BII levels and autophagic flux in wild-type fibroblasts (Fig. 4A, B and C). However, in E193K LRRK2 cells, MPP+ exposure did not significantly modify either autophagosomes basal levels or the autophagic flux (Fig. 4A, B and C). The autophagic activity was also assessed by evaluating P62 protein levels. We observed that the addition of MPP+ toxin did not modify P62 amount in either wild-type cells or E193K LRRK2 fibroblasts. NH₄Cl treatment alone or combined to MPP+ caused the accumulation of P62 protein in both wild-type and E193K lines (Fig. 4D and

To exclude gross damages of the autophagic organelles we measured the levels of Rab7 and the lysosomal associated-membrane protein 2 (LAMP2). Rab7 regulates autophagosome maturation⁵⁵ and LAMP-2 is a key lysosomal protein⁵⁶. We observed that LAMP-2 and Rab7 protein levels were not modified after MPP+ exposure in both wild-type and E193K fibroblasts (Supplementary Figure S5).

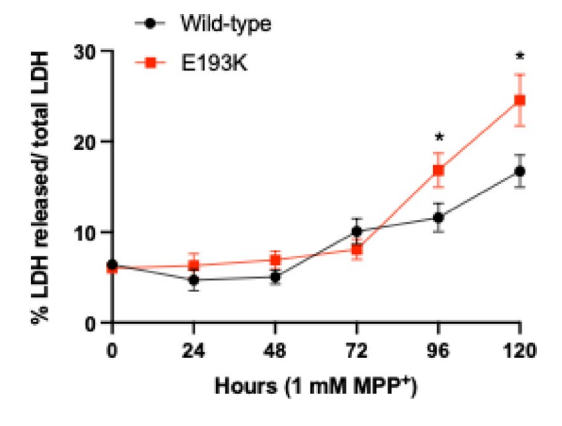


Fig. 3. LRRK2 E193K fibroblasts are more sensitive to MPP⁺ treatment. Human primary fibroblasts collected from a healthy control patient and a E193K LRRK2 carrier were exposed to MPP⁺ (1mM) for several time periods (24 h, 48 h, 72 h, 96 h and 120 h) and cell viability was assessed by the LDH assay. Results are expressed as the percentage of the amount of LDH released to the medium compared to total LDH amount (LDH released plus intracellular LDH amount). Data are expressed as mean \pm SEM; n = 3-5; *p < 0.05. Student's t test.

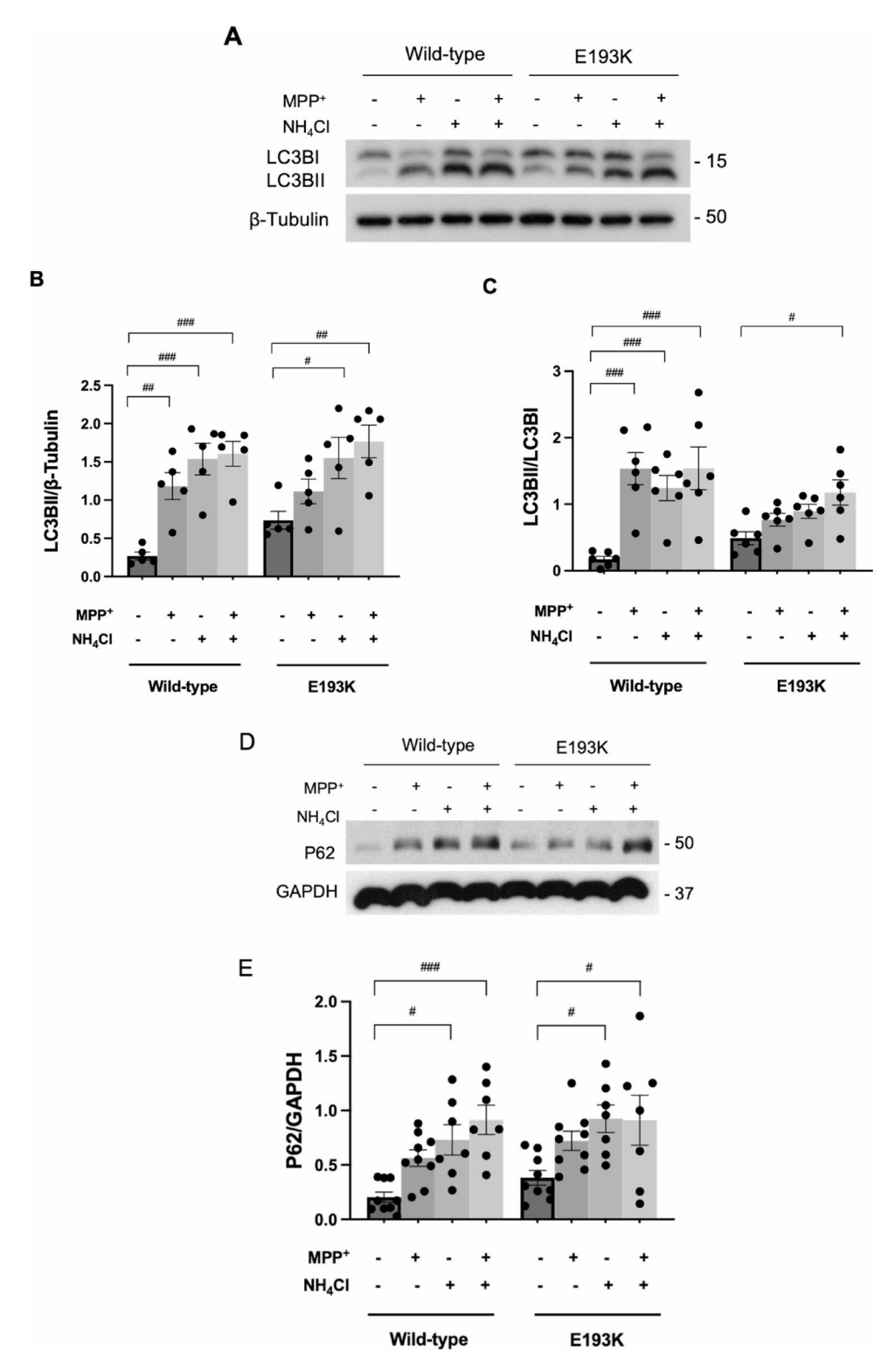


Fig. 4. Autophagic response to MPP⁺ is altered in E193K cells. LC3BI and LC3BII (**A**) and P62 (**D**) protein levels in human primary fibroblasts carrying wild-type or E193K LRRK2 mutation were evaluated by Western-Blot. Cells were treated with NH₄Cl (5mM, 24 h) and/or MPP⁺ (1mM, 24 h) when indicated. The graphs report LC3BII (**B**) and P62 (**E**) protein levels expressed by measuring the optical density of each band and normalized versus β-tubulin or GAPDH amount. (**C**) The graph shows LC3BII/LC3BI ratio by quantification of LC3BII and LCBI bands. LRRK2 (**F**), LC3BI and LC3BII (**H**) protein levels in HEK293 cells overexpressing LRRK2 wild-type and E193K LRRK2 mutation were evaluated by Western-Blot. Cells were treated with MPP⁺ (1mM, 24 h) when indicated. The graphs report LRRK2 (**G**) and LC3BII (**I**) levels expressed by measuring the optical density of each band and normalized versus β-tubulin amount. (**J**) The graph shows LC3BII/LC3BI ratio by quantification of LC3BII and LCBI bands. Data are expressed as mean ± SEM, n = 4–7, #p < 0.05, #p < 0.01, #p < 0.001. Two-way ANOVA.

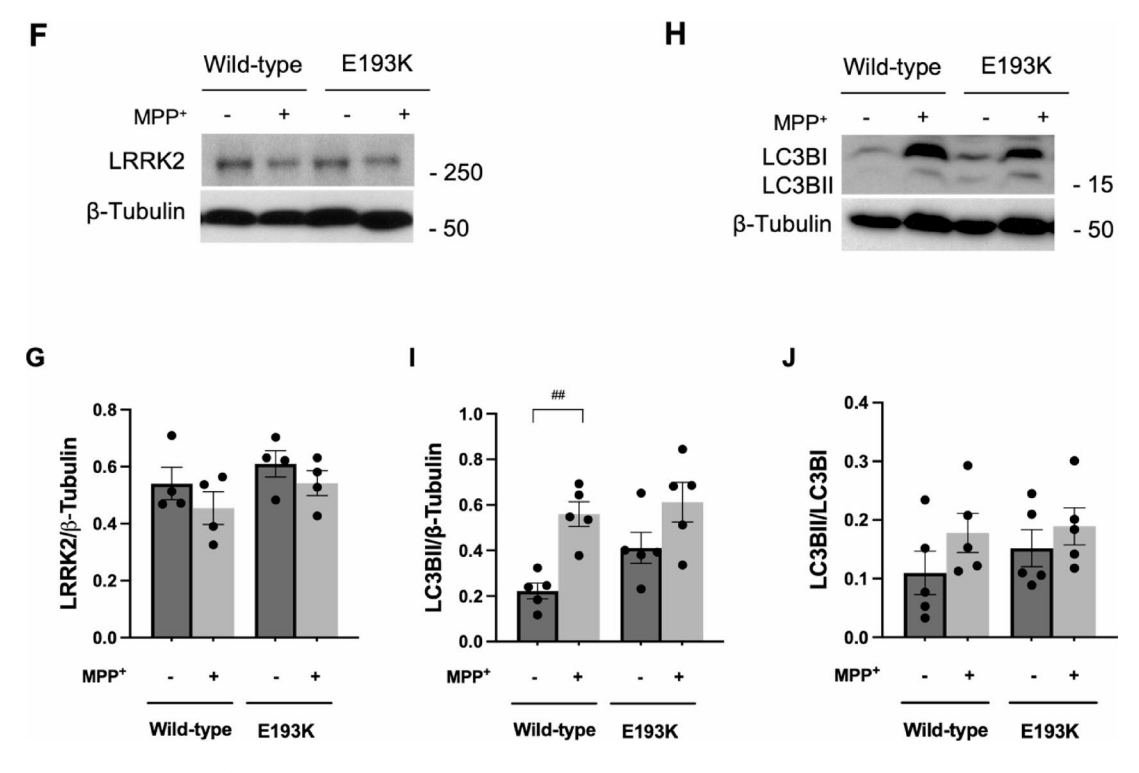


Fig. 4. (continued)

Finally, we studied autophagy in HEK293 cell line upon the overexpression of hLRRK2 wild-type and E193K LRRK2 mutant. While LRRK2 total levels did not change substantially (Fig. 4F and G), we observed that the treatment with MPP+ toxin (1mM, 24 h) triggered autophagy just in wild-type cells, but not in E193K overexpressing cells (Fig. 4H and I). Autophagic flux remained unaffected after MPP+ exposure in both genotypes (Fig. 4H and J). As above, LAMP-2 and Rab7 protein levels were not altered after MPP+ exposure in both wild-type and E193K overexpressing cells (Supplementary Figure S5). These data indicate that MPP+ treatment induces autophagy in wild-type cells but has no major effects in E193K LRRK2 cells.

Discussion

LRRK2 mutations are one of the most common causes of sporadic and familial PD, thus representing an excellent model to understand the molecular mechanisms underlying the pathology⁵⁷. Among LRRK2 variants, we previously described that the E193K mutation leads to the disruption of synaptic vesicle trafficking¹⁷ and mitochondrial dynamics¹⁶. Our present findings show the detrimental impact of the E193K mutation on autophagy. The increment of the autophagy marker LC3BII, suggestive for the deposit of autophagic organelles, characterizes the neurons of PD patients⁵⁸. Applying complementary biochemical and microscopy methods we found that E193K mutation affects autophagy and upon lysosomal blockage, E193K cells show increased amounts of autophagosomes/phagophores. In these conditions, LC3BII and P62 protein clearance was reduced in fibroblasts harbouring the E193K mutation. This indicates that the accumulation of early/immature autophagosomes observed in E193K cells is caused by impaired progression rather than enhanced induction of autophagy. Lysosomal defects may explain inefficient and/or delayed digestion of lysosomal contents. Reduced degradative capacity of lysosomes in G2019S models, for example, has been attributed to lower acidity and increased size of (auto)lysosomes^{59,60}, altered expression of LAMP-2, V-ATPase and cathepsins⁶¹⁻⁶³, as well as to disturbed mannose 6-phosphate receptor (MPR) trafficking and/or disturbed lysosomal reformation 64,65. Whether, and to what extent those factors reported from G2019S cells might contribute to the phenotype observed in E193K cells still remains to be investigated.

Another, mutually not exclusive cause of hampered autolysosomal clearance may relate to the transport of autophagosomes. Nascent autophagosomes move to the perinuclear area^{28,66} and it was shown that impaired retrograde transport and the blockage of autophagosome-lysosome fusion induces autophagosome accumulation and cellular stress^{67,68}. The Dyn-1 complex is critical for the retrograde transport of organelles as autophagosomes^{27,30,69}. The disruption of Dynein-cargo complex impairs axonal transport in neurons leading to degeneration^{70,71}. Among the different subunits of the Dyn-1 complex, Dyn-1 IC is essential for the activation of the motor complex and participates in the binding of Dyn-1 complex to specific cargos⁷². Here we demonstrated that LRRK2 associates to the Dyn-1 complex through the Dyn-1 IC subunit. A previous report described that the kinase domain of LRRK2 interacts with the Dyn-1 complex³². Our data suggest that LRRK2 binding to Dyn-1 IC involves N-terminal and C-terminal parts of the protein. This is not surprising, given that LRRK2 acts as a dimer involving distant interdomain interaction⁷³. Our previous results have demonstrated that the E193K variant modifies LRRK2 biochemical properties and LRRK2 interactome^{16,17}. Accordingly, we found

here that E193K substitution impairs the interaction between LRRK2 and the Dyn-1 complex. This study was conducted in a human primary fibroblast monolayer cell model derived from biopsies of the so far one and only donor carrying this variant¹⁶. Cleary, organelle patterns of non-migrating, unpolarized fibroblasts differ from those of the uniquely shaped neurons. In fibroblasts, distribution of nascent autophagosomes tends to be more diffuse and scattered throughout the cytoplasm, whereas acidic, degradative lysosomes are usually enriched in the perinuclear region. However, finely tuned vectorial, bidirectional transport of autophagic and endo-lysosomal organelles is in any cell type mandatory for successful organelle encounters and fusion⁴⁷. This pertains also to our patient-derived, fibroblasts which still rely on microtubule-based transport and dyneinmediated movement of autophagosomes toward lysosomes and can, therefore, be considered an adequate cell model^{74,75}. We have not studied here the transport of the endo-lysosomal compartments involved, or the possible contribution of adaptors such as Snapin, Rab-interacting lysosomal protein like 1 (RILPL1) or JNKinteracting proteins 3 (JIP3) and 4 (JIP4)^{69,76-80} to the complex autophagic processes, issues that certainly need further investigation. Nevertheless, it can be argued on the basis of our present results, that the E193K variant disrupts the interaction between LRRK2 and the Dyn-1 complex. This provides indirect evidence for affected autophagosome trafficking that, eventually, contributes substantially to the accumulation of autophagic organelles and in turn, compromised autolytic clearance. This notion is also supported by recent data from others on the G2019S LRRK2 mutation^{39,69}, showing defects in directed transport and/or controlled fusion of endosomes and/or lysosomes with autophagosomes to be associated with, or causative for, impaired autolytic clearance. G2019 mutant exhibits increased kinase activity³⁹, instead, E193K variant does not modify LRRK2 kinase activity16 indicating that the observed impairment of autophagy in E193K cells may occur independently of its kinase function.

PD is a complex and multifactorial pathology in which the genetic predisposition combined with specific environmental factors, potentiates the neurodegenerative process. This is the case for the variant G2019S, which enhances the cellular susceptibility to MPP⁺ neurotoxin⁸¹. In line with this idea and our previous results¹⁶, our data indicate that E193K mutation potentiates the cellular sensitivity to MPP+ toxicity and exacerbates the cellular damage. Autophagy is an essential mechanism to guarantee homeostasis and cell survival in response to toxic stimuli. An insufficient autophagic activity could aggravate chemical-induced toxicity⁸². Although previous studies have reported controversial effects of MPP+ on autophagy^{53,83}, in our human fibroblast model we noticed a differential response upon MPP+ exposure in wild-type versus E193K cells. The most recent hypothesis explaining PD pathogenesis is based on the gene x environment theory but additionally, it proposes that the disease arises from the interplay among various contributing factors classified as: triggers (such as environmental toxins), facilitators (like genetic predisposition) and aggravators (such as impaired autophagy)⁴⁴. Our data revealed that MPP+ addition enhances autophagy in LRRK2 wild-type fibroblasts, without any overt effect in E193K harbouring cells. Although we recognize the inherent limitations associated with a specific primary fibroblast line, we successfully replicated our principal findings in a heterologous cell model through over-expression of the LRRK2 E193K variant. The deficient autophagosome maturation or impaired autophagy in E193K LRRK2 fibroblasts may hamper the autophagic response to MPP+ treatment, leading to early autophagic organelle accumulation and autophagic stress. The blockage in autophagy activation may exacerbate the cellular vulnerability to the MPP+ toxin in E193K mutant cells and accelerate cell death (Fig. 5). In neurons, this stress potentially may contribute to the dopaminergic neuronal loss, thereby amplifying or boosting the neurodegeneration and the classical motor symptoms characteristic of the disease.

Conclusions

Our work describes new potential pathological mechanisms related to the E193K LRRK2 mutation, beyond the alteration of synaptic vesicle movement and mitochondrial function. Our data link the alteration of LRRK2 interactome with defects in the autophagic pathway. Our findings highlight the prominent role of LRRK2 as a protein adaptor that regulates autophagosome maturation mediated by the Dyn-1 complex. The E193K variant alters LRRK2-Dyn-1 complex binding and disrupts autophagosome processing, contributing to defective autophagic regulation and thereby, potentiating cellular damage of MPP+ toxin. These advances in the understanding of PD pathogenesis remark the importance of LRRK2 mutations in the regulation of autophagy through the Dyn-1 complex and confirm their essential role in PD pathogenesis in the light of gene x environment theory.

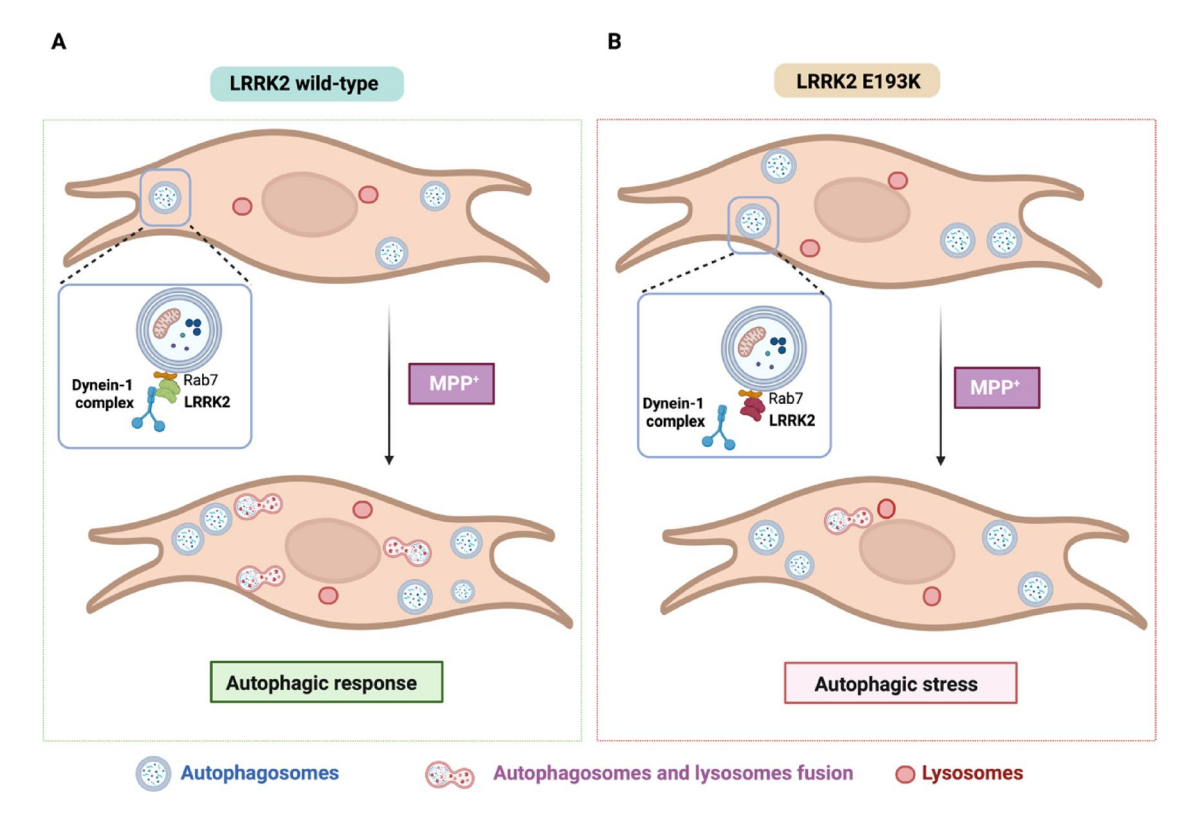


Fig. 5. Schematic representation of autophagy induction by MPP⁺ in LRRK2 wild-type and E193K LRRK mutant cells. (**A**) LRRK2 wild-type interacts with the Dynein-1 complex and allows efficient maturation of autophagosomes under MPP⁺ exposure. (**B**) E193K variant disrupts LRRK2-Dyn-1 complex formation and progression of autophagy under MPP⁺ treatment.

Data availability

The datasets generated during the current study are available from the corresponding author on reasonable request.

Received: 17 April 2025; Accepted: 30 October 2025

Published online: 07 November 2025

References

- 2. Ben-Shlomo, Y. et al. The epidemiology of parkinson's disease. *Lancet* 403, 283–292. https://doi.org/10.1016/S0140-6736(23)0141 9-8 (Jan. 2024).
- 3. Wang, R. & Shih, L. C. Parkinson's disease current treatment. Curr. Opin. Neurol. 36 (4), 302–308. https://doi.org/10.1097/WCO .000000000001166 (Aug. 2023).
- Tolosa, E., Garrido, A., Scholz, S. W. & Poewe, W. Challenges in the diagnosis of parkinson's disease. *Lancet Neurol.* 20 (5), 385–397. https://doi.org/10.1016/S1474-4422(21)00030-2 (May 2021).
- 5. Delamarre, A. & Meissner, W. G. 'Epidemiology, environmental risk factors and genetics of Parkinson's disease', *Presse Médicale*. **46**(2) 175–181. https://doi.org/10.1016/j.lpm.2017.01.001 Mar. (2017).
- 6. Mat Taib, C. N. & Mustapha, M. MPTP-induced mouse model of parkinson's disease: A promising direction of therapeutic
- strategies. Bosn J. Basic. Med. Sci. https://doi.org/10.17305/bjbms.2020.5181 (Dec. 2020).
 7. Blauwendraat, C., Nalls, M. A. & Singleton, A. B. The genetic architecture of parkinson's disease. Lancet Neurol. 19 (2), 170–178.
- https://doi.org/10.1016/S1474-4422(19)30287-X (Feb. 2020).

 8. Ye, H., Robak, L. A., Yu, M., Cykowski, M. & Shulman, J. M. Genetics and pathogenesis of parkinson's syndrome. *Annu. Rev. Pathol. Mech. Dis.* 18 (1), 95–121. https://doi.org/10.1146/annurev-pathmechdis-031521-034145 (Jan. 2023).
- 9. Otmani, H. E., Daghi, M., Jouti, N. T. & Lesage, S. 'An Overview of the Worldwide Distribution of *LRRK2* Mutations in Parkinson's Disease', *Neurodegener. Dis. Manag.* 13(6): 335–350. https://doi.org/10.2217/nmt-2023-0025 Dec. (2023)
- Gloeckner, C. J. & Porras, P. Guilt-by-Association Functional insights gained from studying the LRRK2 interactome. Front. Neurosci. 14, 485. https://doi.org/10.3389/fnins.2020.00485 (May 2020).
- 11. Verma, A. et al. In Silico comparative analysis of LRRK2 interactomes from brain, kidney and lung. *Brain Res.* 1765, 147503. https://doi.org/10.1016/j.brainres.2021.147503 (Aug. 2021).
- 12. Usmani, A., Shavarebi, F. & Hiniker, A. The cell biology of LRRK2 in parkinson's disease. *Mol. Cell. Biol.* 41 (5), e00660–e00620. https://doi.org/10.1128/MCB.00660-20 (May 2021).
- 13. Gilks, W. P. et al. Jan., 'A common LRRK2 mutation in idiopathic Parkinson's disease', *The Lancet.* **365**(9457): 415–416. https://doi.org/10.1016/S0140-6736(05)17830-1 (2005).
- 14. Healy, D. G. et al. Phenotype, genotype, and worldwide genetic penetrance of LRRK2-associated parkinson's disease: a case-control study. *Lancet Neurol.* 7 (7), 583–590. https://doi.org/10.1016/S1474-4422(08)70117-0 (July 2008).

- 15. Bailey, H. M. & Cookson, M. R. How parkinson's Disease-Linked LRRK2 mutations affect different CNS cell types. J. Park Dis. 1-22. https://doi.org/10.3233/JPD-230432 (June 2024).
- 16. Perez Carrion, M. et al. The LRRK2 variant E193K prevents mitochondrial fission upon MPP+Treatment by altering LRRK2 binding to DRP1. Front. Mol. Neurosci. 11, 64. https://doi.org/10.3389/fnmol.2018.00064 (Feb. 2018).
- 17. Marku, A. et al. The LRRK2 N-terminal domain influences vesicle trafficking: impact of the E193K variant. Sci. Rep. 10 (1), 3799. https://doi.org/10.1038/s41598-020-60834-5 (Dec. 2020).
- 18. Nechushtai, L., Frenkel, D. & Pinkas-Kramarski, R. 'Autophagy in Parkinson's Disease', Biomolecules. 13(10): 1435, https://doi.org/ 10.3390/biom13101435 Sept. (2023).
- 19. Li, Y. Y., Qin, Z. H. & Sheng, R. The multiple roles of autophagy in neural function and diseases. Neurosci. Bull. 40 (3), 363-382. https://doi.org/10.1007/s12264-023-01120-y (Mar. 2024).
- 20. Filimonenko, M. et al. Nov., 'Functional multivesicular bodies are required for autophagic clearance of protein aggregates associated with neurodegenerative disease, J. Cell Biol., vol. 179, no. 3, pp. 485-500, (2007). https://doi.org/10.1083/jcb.200702115
- 21. Jahreiss, L., Menzies, F. M. & Rubinsztein, D. C. 'The Itinerary of Autophagosomes: From Peripheral Formation to Kiss-and-Run Fusion with Lysosomes', Traffic, vol. 9, no. 4, pp. 574-587, Apr. (2008). https://doi.org/10.1111/j.1600-0854.2008.00701.x
- Pérez-Carrión, M. D., Posadas, I., Solera, J. & Ceña, V. LRRK2 and proteostasis in parkinson's disease. Int. J. Mol. Sci. 23 (12), 6808. https://doi.org/10.3390/ijms23126808 (June 2022).
- Manzoni, C. & Lewis, P. A. 'LRRK2 and Autophagy', in Leucine-Rich Repeat Kinase 2 (LRRK2), vol. 14, H. J. Rideout, Ed., in Advances in Neurobiology, vol. 14., Cham: Springer International Publishing, pp. 89-105. (2017). https://doi.org/10.1007/978-3-3
- 24. Albanese, F., Novello, S. & Morari, M. Autophagy and LRRK2 in the aging brain. Front. Neurosci. 13, 1352. https://doi.org/10.338 9/fnins.2019.01352 (Dec. 2019).
- Roosen, D. A. & Cookson, M. R. LRRK2 at the interface of autophagosomes, endosomes and lysosomes. Mol. Neurodegener. 11 (1), 73. https://doi.org/10.1186/s13024-016-0140-1 (Dec. 2016)
- 26. Köchl, R., Hu, X. W., Chan, E. Y. W. & Tooze, S. A. 'Microtubules Facilitate Autophagosome Formation and Fusion of Autophagosomes with Endosomes', Traffic, vol. 7, no. 2, pp. 129-145, Feb. (2006). https://doi.org/10.1111/j.1600-0854.2005.00368.x
- 27. Kimura, S., Noda, T. & Yoshimori, T. Dynein-dependent movement of autophagosomes mediates efficient encounters with
- lysosomes. Cell. Struct. Funct. 33 (1), 109–122. https://doi.org/10.1247/csf.08005 (2008). Jia, R., Guardia, C. M., Pu, J., Chen, Y. & Bonifacino, J. S. 'BORC coordinates encounter and fusion of lysosomes with autophagosomes', Autophagy, vol. 13, no. 10, pp. 1648-1663, Oct. (2017). https://doi.org/10.1080/15548627.2017.1343768
- 29. Sidibe, D. K., Vogel, M. C. & Maday, S. Organization of the autophagy pathway in neurons. Curr. Opin. Neurobiol. 75, 102554. https://doi.org/10.1016/j.conb.2022.102554 (Aug. 2022).
- 30. Nambiar, A. & Manjithaya, R. Driving autophagy the role of molecular motors. J. Cell. Sci. 137 (3), jcs260481. https://doi.org/10 .1242/jcs.260481 (Feb. 2024).
- 31. Yildiz, A., Zhao, Y. & 'Dyneins' Curr. Biol., 33, 24, R1274-R1279, doi: https://doi.org/10.1016/j.cub.2023.10.064.Dec. (2023).
- 32. Deniston, C. K. et al. Structure of LRRK2 in parkinson's disease and model for microtubule interaction. Nature 588 (7837), 344-349. https://doi.org/10.1038/s41586-020-2673-2 (Dec. 2020).
- Gloeckner, C. J. et al. Jan., 'The Parkinson disease causing LRRK2 mutation I2020T is associated with increased kinase activity', Hum. Mol. Genet., vol. 15, no. 2, pp. 223-232, (2006). https://doi.org/10.1093/hmg/ddi439
- 34. Gloeckner, C. J., Boldt, K., Schumacher, A., Roepman, R. & Ueffing, M. 'A novel tandem affinity purification strategy for the efficient isolation and characterisation of native protein complexes, PROTEOMICS, vol. 7, no. 23, pp. 4228-4234, Dec. (2007). https://doi.org/10.1002/pmic.200700038
- Piccoli, G. et al. Leucine-Rich repeat kinase 2 binds to neuronal vesicles through protein interactions mediated by its C-Terminal WD40 domain. Mol. Cell. Biol. 34 (12), 2147-2161. https://doi.org/10.1128/MCB.00914-13 (June 2014).
- 36. Pérez-Carrión, M. D. et al. Jan., 'Dendrimer-mediated siRNA delivery knocks down Beclin 1 and potentiates NMDA-mediated toxicity in rat cortical neurons: Autophagy protects from excitotoxicity', J. Neurochem., vol. 120, no. 2, pp. 259-268, (2012). https:/ /doi.org/10.1111/j.1471-4159.2011.07556.x
- 37. Hess, M. W. & Huber, L. A. 'Measuring lysosomal size and frequency by electron microscopy', in Methods in Cell Biology, vol. 164, Elsevier, 47-61. doi: https://doi.org/10.1016/bs.mcb.2020.10.019. (2021).
- Gruenberg, J. 'Life in the lumen: The multivesicular endosome', Traffic, vol. 21, no. 1, pp. 76-93, Jan. (2020). https://doi.org/10.111 1/tra 1271
- 39. Boecker, C. A., Goldsmith, J., Dou, D., Cajka, G. G. & Holzbaur, E. L. F. Increased LRRK2 kinase activity alters neuronal autophagy by disrupting the axonal transport of autophagosomes. Curr. Biol. 31 (10), 2140-2154. https://doi.org/10.1016/j.cub.2021.02.061 (May 2021).
- 40. Zhao, Y. et al. Jan., 'Tissue specific LRRK2 interactomes reveal a distinct striatal functional unit', PLOS Comput. Biol..19(1). e1010847, (2023). https://doi.org/10.1371/journal.pcbi.1010847
- 41. Meixner, A. et al. Jan., 'A QUICK Screen for Lrrk2 Interaction Partners Leucine-rich Repeat Kinase 2 is Involved in Actin Cytoskeleton Dynamics', Mol. Cell. Proteomics, vol. 10, no. 1, p. M110.001172, (2011). https://doi.org/10.1074/mcp.M110.001172
- 42. Zhang, X. & Kortholt, A. 'LRRK2 Structure-Based Activation Mechanism and Pathogenesis', Biomolecules, vol. 13, no. 4, p. 612, Mar. (2023). https://doi.org/10.3390/biom13040612
- Cannon, J. R. & Greenamyre, J. T. Gene-environment interactions in parkinson's disease: specific evidence in humans and mammalian models. Neurobiol. Dis. 57, 38-46. https://doi.org/10.1016/j.nbd.2012.06.025 (Sept. 2013).
- 44. Johnson, M. E., Stecher, B., Labrie, V., Brundin, L. & Brundin, P. Triggers, Facilitators, and aggravators: redefining parkinson's disease pathogenesis. Trends Neurosci. 42 (1), 4-13. https://doi.org/10.1016/j.tins.2018.09.007 (Jan. 2019).
- Gutierrez, M. G., Munafó, D. B., Berón, W. & Colombo, M. I. Rab7 is required for the normal progression of the autophagic pathway in mammalian cells. J. Cell. Sci. 117 (13), 2687-2697. https://doi.org/10.1242/jcs.01114 (June 2004).
- Alegre-Abarrategui, J. et al. Nov., 'LRRK2 regulates autophagic activity and localizes to specific membrane microdomains in a novel human genomic reporter cellular model, Hum. Mol. Genet.. 18(21): 4022-4034, (2009). https://doi.org/10.1093/hmg/ddp346
- Jahreiss, L., Menzies, F. M. & Rubinsztein, D. C. 'The Itinerary of Autophagosomes: From Peripheral Formation to Kiss-and-Run Fusion with Lysosomes', Traffic. 9(4): 574-587. https://doi.org/10.1111/j.1600-0854.2008.00701.x Apr. (2008)
- Klionsky, D. J. et al. Jan., 'Guidelines for the use and interpretation of assays for monitoring autophagy (4th edition) 1', Autophagy, vol. 17, no. 1, pp. 1-382, (2021). https://doi.org/10.1080/15548627.2020.1797280
- 49. Mizushima, N., Yoshimori, T. & Levine, B. 'Methods in Mammalian Autophagy Research', Cell. 140(3): 313-326. https://doi.org/1 0.1016/j.cell.2010.01.028 Feb. (2010).
- Kimura, S., Noda, T. & Yoshimori, T. 'Dissection of the Autophagosome Maturation Process by a Novel Reporter Protein, Tandem Fluorescent-Tagged LC3', Autophagy. 3(5): 452-460. https://doi.org/10.4161/auto.4451 Sept. (2007).
- 51. Dagda, R., Banerjee, T. & Janda, E. How Parkinsonian Toxins Dysregulate the Autophagy Machinery', Int. J. Mol. Sci., vol. 14, no. 11, pp. 22163-22189, Nov. (2013). https://doi.org/10.3390/ijms141122163
- 52. De, A. et al. Dec., 'An optimized protocol for immuno-electron microscopy of endogenous LC3', Autophagy. 18(12): 3004-3022. https://doi.org/10.1080/15548627.2022.2056864 (2022).
- Miyara, M., Kotake, Y., Tokunaga, W., Sanoh, S. & Ohta, S. Mild MPP + exposure impairs autophagic degradation through a novel lysosomal acidity-independent mechanism. J. Neurochem. 139 (2), 294–308. https://doi.org/10.1111/jnc.13700 (Oct. 2016).

- Singh, B. & Bhaskar, S. 'Methods for Detection of Autophagy in Mammalian Cells', Methods Mol. Biol. Clifton NJ. 245–258, 2019. https://doi.org/10.1007/7651 2018 190 (2045).
- 55. Kuchitsu, Y. & Fukuda, M. 'Revisiting Rab7 Functions in Mammalian Autophagy: Rab7 Knockout Studies', Cells, vol. 7, no. 11, p. 215, Nov. (2018). https://doi.org/10.3390/cells7110215
- Eskelinen, E. L. Roles of LAMP-1 and LAMP-2 in lysosome biogenesis and autophagy. Mol. Aspects Med. 27, 5–6. https://doi.org/ 10.1016/j.mam.2006.08.005 (Oct. 2006).
- 57. Sosero, Y. L. & Gan-Or, Z. LRRK2 and parkinson's disease: from genetics to targeted therapy. *Ann. Clin. Transl Neurol.* **10** (6), 850–864. https://doi.org/10.1002/acn3.51776 (June 2023).
- 58. Haik, K. L. et al. Apr., '7-nitroindazole attenuates 6-hydroxydopamine-induced spatial learning deficits and dopamine neuron loss in a presymptomatic animal model of Parkinson's disease,' Exp. Clin. Psychopharmacol., vol. 16, no. 2, pp. 178–189, (2008). https://doi.org/10.1037/1064-1297.16.2.178
- 59. Bravo-San, J. M. et al. The LRRK2 G2019S mutant exacerbates basal autophagy through activation of the MEK/ERK pathway. *Cell. Mol. Life Sci.* 70 (1), 121–136. https://doi.org/10.1007/s00018-012-1061-y (Jan. 2013).
- 60. Henry, A. G. et al. Nov., 'Pathogenic LRRK2 mutations, through increased kinase activity, produce enlarged lysosomes with reduced degradative capacity and increase ATP13A2 expression', *Hum. Mol. Genet.*, vol. 24, no. 21, pp. 6013–6028, (2015). https://doi.org/10.1093/hmg/ddv314
- 61. Klaver, A. C., Coffey, M. P., Aasly, J. O. & Loeffler, D. A. CSF lamp2 concentrations are decreased in female parkinson's disease patients with LRRK2 mutations. *Brain Res.* 1683, 12–16. https://doi.org/10.1016/j.brainres.2018.01.016 (Mar. 2018).
- 62. Wallings, R., Connor-Robson, N. & Wade-Martins, R. 'LRRK2 interacts with the vacuolar-type H+-ATPase pump al subunit to regulate lysosomal function', *Hum. Mol. Genet.*. 28(16): 2696–2710. https://doi.org/10.1093/hmg/ddz088 Aug. (2019).
- 63. Yadavalli, N. & Ferguson, S. M. 'LRRK2 suppresses lysosome degradative activity in macrophages and microglia through MiT-TFE transcription factor inhibition', *Proc. Natl. Acad. Sci.*, vol. 120, no. 31, p. e2303789120, Aug. (2023). https://doi.org/10.1073/pnas.2 303789120
- 64. MacLeod, D. A. et al. Feb., 'RAB7L1 Interacts with LRRK2 to Modify Intraneuronal Protein Sorting and Parkinson's Disease Risk', *Neuron*, vol. 77, no. 3, pp. 425–439, (2013). https://doi.org/10.1016/j.neuron.2012.11.033
- Magalhaes, J. et al. Autophagic lysosome reformation dysfunction in glucocerebrosidase deficient cells: relevance to Parkinson disease. Hum. Mol. Genet. 25 (16), 3432–3445. https://doi.org/10.1093/hmg/ddw185 (Aug. 2016).
- Maday, S., Wallace, K. E. & Holzbaur, E. L. F. Autophagosomes initiate distally and mature during transport toward the cell Soma in primary neurons. J. Cell. Biol. 196 (4), 407–417. https://doi.org/10.1083/jcb.201106120 (Feb. 2012).
- 67. Heerssen, H. M., Pazyra, M. F. & Segal, R. A. Dynein motors transport activated Trks to promote survival of target-dependent neurons. *Nat. Neurosci.* 7 (6), 596–604. https://doi.org/10.1038/nn1242 (June 2004).
- 68. Xu, M. et al. Blocking retrograde axonal transport of autophagosomes contributes to sevoflurane-induced neuron apoptosis in APP/PS1 mice. *Acta Neurol. Belg.* **121** (5), 1207–1215. https://doi.org/10.1007/s13760-020-01359-6 (Oct. 2021).
- 69. Cason, S. E. & Holzbaur, E. L. F. 'Axonal transport of autophagosomes is regulated by dynein activators JIP3/JIP4 and ARF/RAB GTPases', J. Cell Biol.. 222(12): e202301084. https://doi.org/10.1083/jcb.202301084 Dec. (2023).
- 70. LaMonte, B. H. et al. May., 'Disruption of Dynein/Dynactin Inhibits Axonal Transport in Motor Neurons Causing Late-Onset Progressive Degeneration', *Neuron.* 34(5): 715–727. https://doi.org/10.1016/S0896-6273(02)00696-7 (2002).
- Bejarano, E. et al. Defective recruitment of motor proteins to autophagic compartments contributes to autophagic failure in aging.
 Aging Cell. 17 (4), e12777. https://doi.org/10.1111/acel.12777 (Aug. 2018).
- 72. Nurminsky, D. I. et al. 'Cytoplasmic Dynein Intermediate-Chain Isoforms with Different Targeting Properties Created by Tissue-Spacific Alternative Splicing Mod. Cell. Biol. 19(11), 6916, 6915, https://doi.org/10.1109/MCP.19.11.6916 Nov. (1009)
- Specific Alternative Splicing, Mol. Cell. Biol.. 18(11): 6816–6825. https://doi.org/10.1128/MCB.18.11.6816 Nov. (1998).

 73. Guaitoli, G. et al. July, 'Structural model of the dimeric Parkinson's protein LRRK2 reveals a compact architecture involving distant
- interdomain contacts', *Proc. Natl. Acad. Sci.*. **113**(30): E4357–E4366. https://doi.org/10.1073/pnas.1523708113 (2016)
 74. Di Bartolomeo, S. et al. Oct., 'The dynamic interaction of AMBRA1 with the dynein motor complex regulates mammalian
- autophagy', J. Cell Biol., vol. 191, no. 1, pp. 155–168, (2010). https://doi.org/10.1083/jcb.201002100
 75. Tempes, A. et al. Autophagy initiation triggers p150Glued–AP-2β interaction on the lysosomes and facilitates their transport. Cell. Mol. Life Sci. 81 (1). https://doi.org/10.1007/s00018-024-05256-6 (Dec. 2024).
- Celestino, R. et al. JIP3 interacts with dynein and kinesin-1 to regulate bidirectional organelle transport. J. Cell. Biol. 221 (8). https://doi.org/10.1083/jcb.202110057 (Aug. 2022).
- 77. Cai, Q. et al. Snapin-Regulated Late Endosomal Transport Is Critical for Efficient Autophagy-Lysosomal Function in Neurons', Neuron. 68(1): 73-86. https://doi.org/10.1016/j.neuron.2010.09.022 Oct. (2010).
- Jordens, I. et al. Oct., 'The Rab7 effector protein RILP controls lysosomal transport by inducing the recruitment of dynein-dynactin motors', Curr. Biol.. 11(21): 1680–1685. https://doi.org/10.1016/S0960-9822(01)00531-0 (2001).
- Willett, R. et al. 'TFEB regulates lysosomal positioning by modulating TMEM55B expression and JIP4 recruitment to lysosomes', Nat. Commun. 8(1): 1580. https://doi.org/10.1038/s41467-017-01871-z Nov. (2017).
- Boecker, C. A. & Holzbaur, E. L. F. Hyperactive LRRK2 kinase impairs the trafficking of axonal autophagosomes, *Autophagy. Aug* 17 (8), 2043–2045. https://doi.org/10.1080/15548627.2021.1936933 (2021).
- 81. Yakhine-Diop, S. M. S. et al. G2019S LRRK2 mutant fibroblasts from parkinson's disease patients show increased sensitivity to neurotoxin 1-methyl-4-phenylpyridinium dependent of autophagy', *Toxicology. Oct* 324, 1–9. https://doi.org/10.1016/j.tox.2014.0 7.001 (2014).
- 82. Pesonen, M. & Vähäkangas, K. Autophagy in exposure to environmental chemicals. *Toxicol. Lett.* **305**, 1–9. https://doi.org/10.1016/j.toxlet.2019.01.007 (May 2019).
- 83. Azam, S. et al. Apr., 'Dioscin-Mediated Autophagy Alleviates MPP+-Induced Neuronal Degeneration: An In Vitro Parkinson's Disease Model', *Molecules*. 27(9): 2827. https://doi.org/10.3390/molecules27092827 (2022).

Acknowledgements

The authors thank Vanesa Guijarro, Karin Gutleben, Ruth Joas and Barbara Witting for their support and technical assistance, the "Cell line and DNA biobank from patients affected by genetic diseases" (Istituto G. Gaslini) and "Parkinson Institute Biobank" (Milan, www.parkinson.it/biobanca.html), both members of the Telethon Network of Genetic Biobanks funded by Telethon Italy (http://www.biobanknetwork.org, project No.GTB12001).

Author contributions

S.R.: methodology, formal analysis, writing-review and editing. F.Z.: methodology. C. J. G.: formal analysis, writing-review and editing. I.P.: writing—original draft, writing-review and editing. V.C.: writing-review, editing and funding acquisition. M. W. H.: formal analysis and data curation, writing—original draft, writing-review and editing. G.P.: conceptualization, writing—original draft, writing-review, editing and funding acquisition. M.D.P-C.: methodology, formal analysis, writing—original draft, writing-review and editing, funding acquisition.

Funding

This study was financially supported by the Research and Innovation Agency of Castilla-La Mancha (grant number SBPLY/19/180501/000060) to María Dolores Pérez-Carrión, by MUR-PRIN 20222LRHCW to Giovanni Piccoli, by Ministry of Science, Innovation and Universities and JCCM with funding from European Union NextGenerationEU (PRTR-C17.I1) and by the University of Castilla-La Mancha project 2022-GRIN-34370 to Valentín Ceña. Grant number (SBPLY/23/180225/000022) was granted by Research and Innovation Agency of Castilla-La Mancha to María Dolores Pérez-Carrión. Grant number (DIPUAB-2021-5) was granted by the Diputación provincial de Albacete and by the University of Castilla-La Mancha to María Dolores Pérez-Carrión.

Competing interests

The authors declare no competing interests.

Competing interests

The authors declare no competing interests.

Ethics approval

This study was approved by the Ethical Committee "Comitato Etico Milano Area C" on the 26/06/2015 (Numero Registro dei pareri: 370-062015) and was conducted according to the Declaration of Helsinki and to the Italian legislation. Written informed consent was obtained from all participants.

Additional information

Supplementary Information The online version contains supplementary material available at https://doi.org/1 0.1038/s41598-025-26716-4.

Correspondence and requests for materials should be addressed to M.D.P.-C.

Reprints and permissions information is available at www.nature.com/reprints.

Publisher's note Springer Nature remains neutral with regard to jurisdictional claims in published maps and institutional affiliations.

Open Access This article is licensed under a Creative Commons Attribution-NonCommercial-NoDerivatives 4.0 International License, which permits any non-commercial use, sharing, distribution and reproduction in any medium or format, as long as you give appropriate credit to the original author(s) and the source, provide a link to the Creative Commons licence, and indicate if you modified the licensed material. You do not have permission under this licence to share adapted material derived from this article or parts of it. The images or other third party material in this article are included in the article's Creative Commons licence, unless indicated otherwise in a credit line to the material. If material is not included in the article's Creative Commons licence and your intended use is not permitted by statutory regulation or exceeds the permitted use, you will need to obtain permission directly from the copyright holder. To view a copy of this licence, visit http://creativecommons.org/licenses/by-nc-nd/4.0/.

© The Author(s) 2025